J. Fluid Mech. (1966), *vol.* 26, *part* 1, *pp.* 37–47
Printed in Great Britain

Grid turbulence at large Reynolds numbers†

By A. L. KISTLER AND T. VREBALOVICH
Jet Propulsion Laboratory, Pasadena, California

(Received 24 November 1965)

Measurements of grid turbulence have been obtained for grid Reynolds numbers ranging from $2\cdot4 \times 10^6$ to $1\cdot2 \times 10^5$. The decay law and the effect of Reynolds number on the turbulence level are established. The measured power spectra of the turbulence are consistent with Kolmogoroff scaling for $k\eta > 0\cdot1$ (k is the wave-number and η is the Kolmogoroff length); but for $k\eta < 0\cdot1$, the spectra of the stream-wise turbulence velocity component and of the cross-stream component do not appear to be isotropically related. However, the stream-wise spectrum does display a $-\frac{5}{3}$ region, which increases in extent with increasing Reynolds number.

1. Introduction

The turbulent flow downstream of a grid of moderate solidity placed perpendicular to a uniform stream has two features which make it particularly useful for the study of turbulence structure.

The first is that this flow field consists of the collection of wakes behind the obstacles comprising the grid. Sufficiently far downstream, these wakes coalesce, and the turbulence has statistical properties that are approximately uniform in a plane perpendicular to the stream direction (parallel to the grid). As a consequence, the change in the average properties of the turbulence with distance from the grid is controlled primarily by dissipation, and the rate of dissipation can be easily obtained by measuring the change in the level of the turbulent fluctuation as a function of distance from the grid. The pressure-velocity work, the other term appearing in the energy equation, is believed to be negligible for the small turbulence levels encountered in these flows.

The second important feature of this flow is that measurements of the fluctuation velocity as a function of time at a fixed point in space can be related to the spatial structure of the turbulence with good accuracy through the relation $\Delta x = U_0 \Delta t$ (Favre, Gaviglio & Dumas 1953), where x is the stream-wise length co-ordinate, t the time, and U_0 the mean stream velocity. This relation, which implies that the pattern of disturbance in the flow (eddies) is carried along with the local mean velocity, is a good approximation when the mean velocity does not change appreciably over distances comparable to the scale of the turbulence, and when the turbulence level is small. Grid turbulence satisfies both requirements.

During the last few days in the life of the Southern California Co-operative Wind

† This paper presents the results of one phase of research carried out at the Jet Propulsion Laboratory, California Institute of Technology, under Contract No. NAS 7-100, sponsored by the National Aeronautics and Space Administration.

Tunnel (CWT), these features of grid turbulence were used to examine the range of usefulness of Kolmogoroff's theories of the structure of turbulence at larger Reynold's numbers. The theories deal with the small-scale components of the turbulent motion, a region most easily examined through spectral measurements in conjunction with a space-time transformation.

The CWT was a large tunnel which could be operated at high speeds and high densities so that grid turbulence could be generated at reasonably large Reynolds numbers. The Reynolds number could be varied by changing the density alone, so that one could obtain the effect of Reynolds-number change on the data without modifying the grid size or the space-time transformation. This possibility simplified spectral measurements, since the frequency range of the measurements does not change drastically when the Reynolds number is changed.

Because the data were taken shortly before the CWT ceased operation, time was limited and there was no possibility of checking measurements to clarify any unusual features that emerged in the analysis of the data. For this reason, only a few of these results were reported earlier in a brief abstract (Kistler & Vrebalovich 1961). Since that time, other work on grid turbulence has given evidence in their support, and it is felt that publication of the complete results is warranted.

2. Experimental equipment

The Co-operative Wind Tunnel was a closed-circuit facility with a working section $8{\cdot}5 \times 11{\cdot}5$ ft. in cross-section and a uniform mean flow over a length of 35 ft. The temperature rise produced by the fans which drive the stream is removed by a water-cooled heat exchanger spanning the settling chamber. This cooling system introduces a temperature non-uniformity into the flow. Hot-wire measurements of the combined temperature and velocity fluctuations in the working section without the grid showed, however, that these fluctuations correspond, in terms of hot-wire signal, to a velocity-fluctuation level of less than $0{\cdot}1\%$.

A bi-plane, square-mesh grid made of 1·25 in.-diameter pipe, spaced 6·75 in. from centre to centre, was installed normal to the stream direction at the upstream end of the working section. The grid solidity was 0·335. The hot-wire for measuring the fluctuations and a Pitot tube for measuring the dynamic pressure were mounted near the tunnel centre-line on a traversing mechanism. This traverse could move the measuring probes 5 ft. along the centre-line as well as 6 in. normal to the stream direction. The traverse could rotate a hot-wire probe in the horizontal plane to permit direct calibration of a hot-wire for measuring v', the cross-stream component of the turbulence.

The hot wires were 0·00005 in.-diameter, 90 % platinum–10 % rhodium wires of 0·014 in. length. A single wire normal to the stream was used to measure u', the stream-wise turbulence component, and two wires in an 'X' configuration with an included angle of about 75° were used to measure v'. The constant-current hot-wire set† had a compensated frequency response up to 100 kcycles for the time constants encountered. The capacity of the 170 ft. cable connecting the hot wires to the

† Shapiro and Edwards Model A 50.

amplifier, in conjunction with the hot-wire resistance, produced no significant attenuation to the signal below 500 kcycles.

The power spectra of the hot-wire signals were obtained with a Hewlett–Packard 300 A wave analyser for the frequency range from 20 cycles/sec to 16 kcycles, and with a Sierra 121 wave analyser for the frequency range from 15 to 100 kcycles. Both analysers use the heterodyne principle and have constant bandwidth. The Hewlett–Packard analyser output contains not only the energy in the neighbourhood of the passband, but also the energy in the neighbourhood of 20 kcycles. A filter was used to suppress the 20 kcycle component, and the data were corrected for the filter characteristics.

3. Test conditions and calibration

All measurements were made near room temperature and at a free-stream velocity of 200 ft./sec. This was near the highest velocity that could be used without introducing significant compressibility effects in the flow over the grid. The grid Reynolds number was varied by changing the pressure level of the tunnel. The available pressure range from 0·2 to 4 atm. corresponded to a range of grid Reynolds number Re_M from $1{\cdot}2\times 10^5$ to $2{\cdot}4\times 10^6$, where $Re_M = U_0 M/\nu$, M is the bar spacing, and ν the kinematic viscosity.

The hot wires were calibrated in the tunnel. Those normal to the stream, used for measuring the stream-wise component of the velocity fluctuations, were calibrated by setting the wire operating conditions at $U_0 = 200$ ft./sec and then changing U_0 over a small range and measuring $\Delta e/\Delta u$, where e is the mean voltage across the wire. With this calibration method, it is not necessary to assume a particular form for the heat-loss laws from fine wires, but the velocity increments must be measured accurately. At high pressures, the velocity increment could be measured without difficulty, but for pressures below 1 atm., the pressure transducers had insufficient resolution to determine U_0 with the necessary accuracy. For these low pressures, the calibration curve of tunnel fan-blade angle versus mean velocity was assumed to be the same as for high pressures, and the velocity was determined from the blade angle.

The 'X' meters for measuring v' were calibrated by rotating the probes in the stream and measuring their angle sensitivity. When the 'X' meters were aligned with the flow, they had negligible u' sensitivity.

4. Measurement errors

In these tests, measurements were made of the turbulent fluctuation levels and of the shapes of the spectra. The accuracy of the fluctuation levels was almost wholly determined by the accuracy of the wire calibration, since the wires were much shorter than the scales of the energy-containing eddies. The wire calibrations are estimated to be within 10 % of the true value for both u' and v', with the highest accuracy at the high pressure levels.

For the low-level turbulence encountered here, the main errors in the measurements of the spectral shapes are caused by the effects of finite wire length l and by errors in setting the time constants τ of the wires. A finite-length hot wire averages the large wave-number components over the wire length, and the contribution of these components to the output voltage is attenuated with respect to the contribution of the small wave-number components. This effect has been calculated for isotropic turbulence (Uberoi & Kovásznay 1953); the correction to the measured spectrum at a point requires a knowledge of the true spectral shape from this point to $k = \infty$, where k is the wave-number of a spectral component. The best that can usually be done is to place a bound on the correction. If the spectrum has a monotonically decreasing logarithmic slope, the effect of the correction is always to decrease this slope. The correction is a function of kl; for the wire length used in these tests, no significant effect is indicated for $k < 28/\text{cm}$. The reported data are not corrected for wire length, since $k = 28/\text{cm}$ was beyond the region of primary interest in all the measurements.

An error in time-constant setting can occur when the square-wave technique is used in a region of large velocity fluctuations. If $E(f)$ is the true one-dimensional frequency spectrum (f is the frequency), τ the true wire time constant, and τ_a the time constant used, the measured power spectrum $E_m(f)$ will be

$$E_m(f) = E(f)\{1+(2\pi\tau_a f)^2\}\{1+(2\pi\tau f)^2\}$$

over the frequency range where the compensation is effective. For $f \ll 1/\tau$, $1/\tau_a$, the measured spectrum is equal to the true spectrum. For $f \gg 1/\tau$, $1/\tau_a$, the measured spectrum has the same shape as the true spectrum, but the amplitudes differ by a factor of $(\tau_a/\tau)^2$. In the intermediate region, both the shape and the level are affected.

In the reasonably low turbulence levels encountered in these tests, the time constant could be set within a few per cent, so that no large error in the slopes or levels is expected from this source. The time constants were approximately 0·1 msec, so that $2\pi\tau f = 1$ at $f = 1{\cdot}6$ kcycles, or at about $k = 2\pi f/U_0 = 1{\cdot}6\,\text{cm}^{-1}$. This wave-number is well below that at which the spectral shape is of particular interest.

5. Fluctuation levels and energy decay

Measurements of the variation of turbulent energy with distance from the grid were obtained for the maximum pressure flow. Insufficient time was available to make such measurements for other conditions. The results obtained at the maximum Reynolds number were similar to those expected at much smaller Reynolds numbers, indicating that the decay law probably does not change over the range of Reynolds numbers considered here.

The determination of the dissipation rate ϵ required the differentiation of the function relating the turbulent energy to the distance from the grid,

$$\epsilon = \frac{1}{2U_0}\frac{d}{dx}(\tilde{u}^2+\tilde{v}^2+\tilde{w}^2),$$

where $\tilde{u}$, $\tilde{v}$ and $\tilde{w}$ are the root-mean-square of the three normal fluctuation components u', v' and w'.

The symmetry of the flow imposes the requirement that the two cross-stream turbulence components have equal mean-square values ($\tilde{v}^2 = \tilde{w}^2$). Therefore,

$$\epsilon = \frac{1}{2U_0}\frac{d}{dx}(\tilde{u}^2 + 2\tilde{v}^2)$$

and the energy per unit mass is $1/2(\tilde{u}^2 + 2\tilde{v}^2)$. This differentiation is carried out by determining an average curve through the experimental points and then differentiating the curve. For a limited range near the grid ($10 < x/M < 100$), it is customary to use the initial period relations

$$\frac{1}{\tilde{u}^2} = A\left(\frac{x}{M} - \frac{x_0}{M}\right), \quad \frac{1}{\tilde{v}^2} = B\left(\frac{x}{M} - \frac{x_1}{M}\right) \qquad (1), (2)$$

to fair the data. The data plotted in this fashion are shown in figure 1. The effective origins, x_0 and x_1, for u' and v' are different but are within the range expected from previous measurements at much smaller Reynolds numbers. The measurements give the usual result that $\tilde{u} > \tilde{v}$, and consequently the turbulence does not satisfy the condition of isotropy.

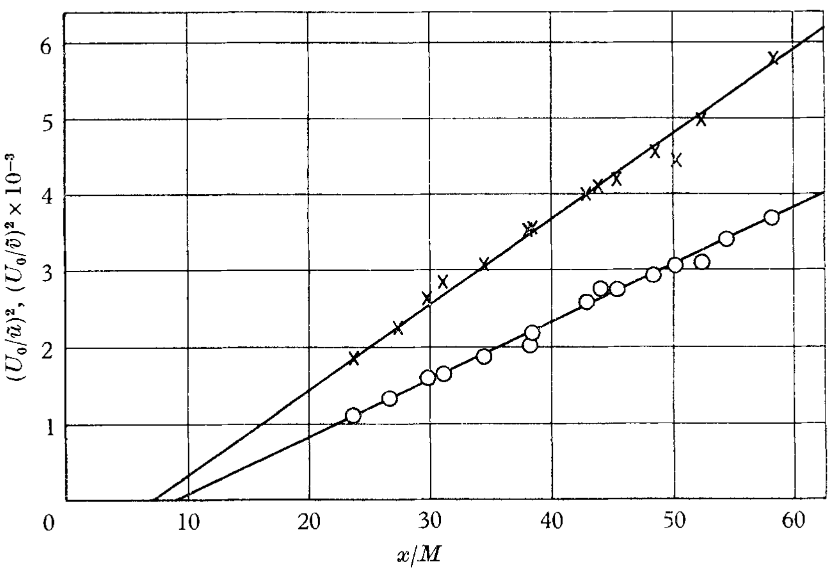

FIGURE 1. The turbulent energy as a function of distance from the grid. The straight lines were used to compute the dissipation rate. ○, $(U_0/\tilde{u})^2$; ×, $(U_0/\tilde{v})^2$.

The form of the decay law is given by the above relation to a reasonable degree of approximation, but the values of A and B in equations (1) and (2) change with the pressure drop across the grid. The power used in pushing the air through the grid appears both as turbulence and as internal energy; if the ratio of the energy going to each energy sink is not sensitive to Reynolds number, then A and B would be expected to be proportional to $1/C_p$. Measurements of $\tilde{u}$ and $\tilde{v}$ as a function of Reynolds number were obtained at $x/M = 45$ and are shown in figure 2 along with the measured pressure-drop coefficient of the grid. The available Reynolds-number range was large enough to span the critical Reynolds number for the grid bars, as is shown by the drop in the measured C_p somewhere between $Re_M = 0{\cdot}7 \times 10^6$ and $1{\cdot}25 \times 10^6$. Both $\tilde{u}$ and $\tilde{v}$ reflect this change in C_p, but $\tilde{u}$ remains larger than $\tilde{v}$ for the entire range of Re_M.

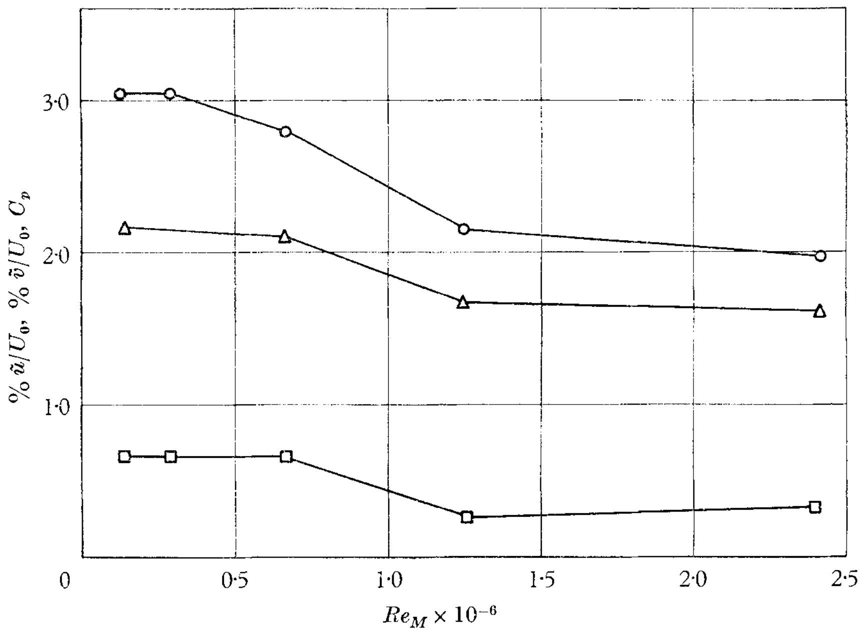

FIGURE 2. The effect of Reynolds number on the grid pressure drop and on the turbulence level at $x/M = 45$, where $Re_M = U_0M/\nu$. ○, $\tilde{u}/U_0$; △, $\tilde{v}/U_0$; □, $C_p = 2\Delta p/\rho U_0^2$.

P (cm Hg)	T_0 (°K)	ν(cm²/sec)	$\tilde{u}/U_0$ (%)	$\tilde{v}/U_0$ (%)	ϵ(cm²/sec³)	L(cm)	η^{-1}(1/cm)	$Re_L = \tilde{u}L/\nu$
295	311	$4{\cdot}31 \times 10^{-2}$	1·97	1·60	$1{\cdot}62 \times 10^5$	4·78	$2{\cdot}12 \times 10^2$	$1{\cdot}33 \times 10^4$
145	302	$8{\cdot}33 \times 10^{-2}$	2·15	1·67	$1{\cdot}84 \times 10^5$	4·78	$1{\cdot}34 \times 10^2$	$7{\cdot}5 \times 10^3$
76	300	$1{\cdot}57 \times 10^{-1}$	2·80	2·1	$3{\cdot}02 \times 10^5$	6·0	$9{\cdot}38 \times 10^1$	$6{\cdot}53 \times 10^3$
15	292	$7{\cdot}6 \times 10^{-1}$	3·05	2·17	$3{\cdot}38 \times 10^5$	6·28	$2{\cdot}96 \times 10^1$	$1{\cdot}54 \times 10^3$
Laufer 1954 (pipe)	—	$1{\cdot}5 \times 10^{-1}$	2·84	—	$2{\cdot}04 \times 10^5$	5·5	$8{\cdot}8 \times 10^1$	$3{\cdot}2 \times 10^3$

TABLE 1. Mean properties of the flow at $x/M = 45$, $U_0 = 6100$ cm/sec, $M = 17{\cdot}15$ cm

If these data are used to evaluate C_pA, a value of about 25 is obtained. The turbulent energy at $x/M = 45$ remains about the same fraction of the expended power on both sides of the critical Reynolds number; namely, about 1 %.

The measured levels and assumed decay law were used to evaluate the dissipation rate at $x/M = 45$, the location at which the spectra were measured. Table 1 shows the values of the important parameters evaluated at that point for the various conditions investigated.

6. Spectra

The power spectra of the hot-wire signals were obtained at $x/M = 45$, where the turbulence length scales were such that the interesting portions of the spectra were within the frequency range of the hot-wire equipment for the complete range of pressure levels. The time spectra of the hot-wire signals were converted to space spectra of the turbulent velocity components by using the wire calibration and the transformation $k = 2\pi f/U_0$.

At least two length scales are needed to characterize the nature of the turbulence; the most meaningful scales for spectra are the outer scale and the Kolmogoroff length. The outer scale is comparable to the scale of the turbulence-producing object (mesh or bar size in our case); the Kolmogoroff length is given by the dissipation rate and the viscosity, and it depends on the Reynolds number of the turbulence as well as the scale of the turbulence-producing object. The outer scale most commonly used for describing grid turbulence, and the one which can be obtained from the measured spectrum itself, is the integral scale. This scale is defined by

$$\tilde{u}^2 L = \int \langle u'(x)\, u'(x+r)\rangle\, dr$$

(where the symbol $\langle\ \rangle$ indicates time average) and, with the space-time transformation, is given by $L = \pi/2E_1(0)$, where E_1 is the area-normalized one-dimensional spectrum of u', i.e.

$$\int_0^\infty E_1(k)\, dk = 1.$$

$E_2(k)$ will be the area-normalized one-dimensional spectrum of v'.

The measured spectra are shown in figure 3. Plotting $E(k)/L$ vs. kL with linear scales emphasizes the small wave-number end of the spectra. The u' spectra are forced to go through the point $E_1(0)/L = 2/\pi$ by the method of computing L. If the turbulence were isotropic, the v' spectra should have an intercept at one-half this value, and this is seen to be approximately true. From previous work on grid turbulence, it is known that the similarity displayed by the u' and the v' spectra, respectively, is a consequence of the fact that the same grid was used in all cases. A different grid or another turbulent flow would not, in general, produce spectra with the same shape at low wave-numbers.

The Kolmogoroff theory states that if the Reynolds number is sufficiently large so that the outer length scale of the turbulence is significantly larger than the inner scale, then the turbulent energy associated with the high wave-number region of the spectra should be isotropically distributed in space. In proper co-ordinates, the spectrum in this region should be a universal function for all turbulent flows. Kolmogoroff also proposed that for sufficiently large Reynolds numbers, a spectral region would exist that was still isotropic, but where the spectral shape depended only on ϵ and not on ν. This inertial subrange would have a spectral shape $E \sim k^{-\frac{5}{3}}$. Using the dissipation rate computed from the decay data, the Kolmogoroff length $\eta = (\nu^3/\epsilon)^{\frac{1}{4}}$ and the Kolmogoroff energy-spectrum scale $E_0 = (\epsilon\nu^5)^{\frac{1}{4}}$ were calculated. The measured u' spectra are plotted in figure 4 in co-ordinates made non-dimensional with these factors. A log-log plot is used, since the interesting region is at large wave numbers, where the energy is small and the spectra decrease rapidly with increasing wave-number. A spectrum measured in a pipe is also shown in figure 4. The dissipation was measured for this spectrum so that η and E_0 could be computed.

The qualitative changes of the spectral shape with Re_L and k are as expected. For $k\eta > 0{\cdot}1$, all of the spectra seem to have the same shape. The extent of the region where $E_1 \sim k^{-\frac{5}{3}}$ $(k\eta < 0{\cdot}1)$ increases with increasing Reynolds number. For the smallest k, the spectra appear to approach a horizontal asymptote.

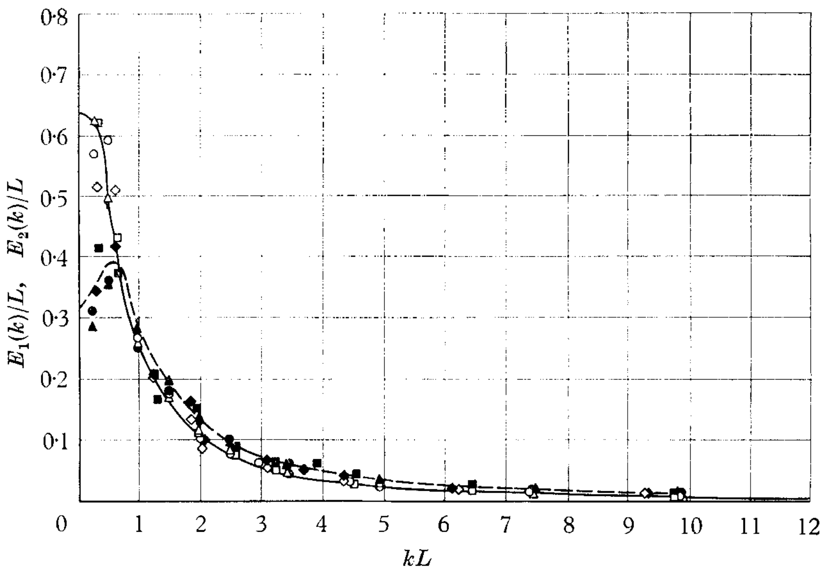

FIGURE 3. The small wave-number portion of the spectra. Both E_1 and E_2 have unit area on this plot.

$E_2(k)$	$E_1(k)$	Re_L
●	○	$13{\cdot}3 \times 10^3$
▲	△	$7{\cdot}5 \times 10^3$
◆	◇	$6{\cdot}5 \times 10^3$
■	□	$1{\cdot}5 \times 10^3$

The value of the $k = 0$ asymptote can be estimated as follows. For turbulent flows in geometrically similar boundaries and in which the dimensionless outer scale and fluctuation levels do not change with Reynolds number, a well-known argument shows that the dissipation rate is given by $\epsilon = D\tilde{u}^3/L$, where D is independent of the Reynolds number and $\tilde{u}$ and L are the stream-wise fluctuation level and integral scale, respectively. The grid turbulence examined here approximately satisfies this relation, even though both $\tilde{u}$ and L change with Re_L. This is the case because with $\tilde{u}/U_0 \sim C_p^{\frac{1}{2}}$, and with the form of the decay law independent of Re_L, D will be constant if $L \sim C_p^{\frac{1}{2}}$, a relationship that approximates the measurement here. With ϵ related to L in this manner, the $k = 0$ intercept of E_1 on a spectral plot in Kolmogoroff variables is $(2/\pi D^{\frac{1}{4}})\, Re_L^{\frac{5}{4}}$. These intercepts are shown in figure 4 with $D = 0{\cdot}4$. This value of D would, of course, be different if some other measure of the fluctuation level were used—e.g. $[(\tilde{u}^2 + 2\tilde{v}^2)/3]^{\frac{1}{2}}$. The same remark applies to the value of Re_L.

Isotropy implies a definite relation between the u' and v' spectra. For regions of the spectra in which a power law is a good approximation to the shape, this relation is particularly simple; i.e. if $E_1 \sim k^{-n}$, then $E_2 = [\frac{1}{2}(1+n)]\, E_1$. When the u' spectra on the log plot are approximated by the straight-line segments shown and the results are transferred over to E_2, the straight lines indicated on figure 5 are obtained.

The measured points of E_2 are too scattered to permit anything more than qualitative statements to be made about the relationship between E_1 and E_2. For $k\eta > 0{\cdot}03$ (approximately), the data are not inconsistent with the prediction of

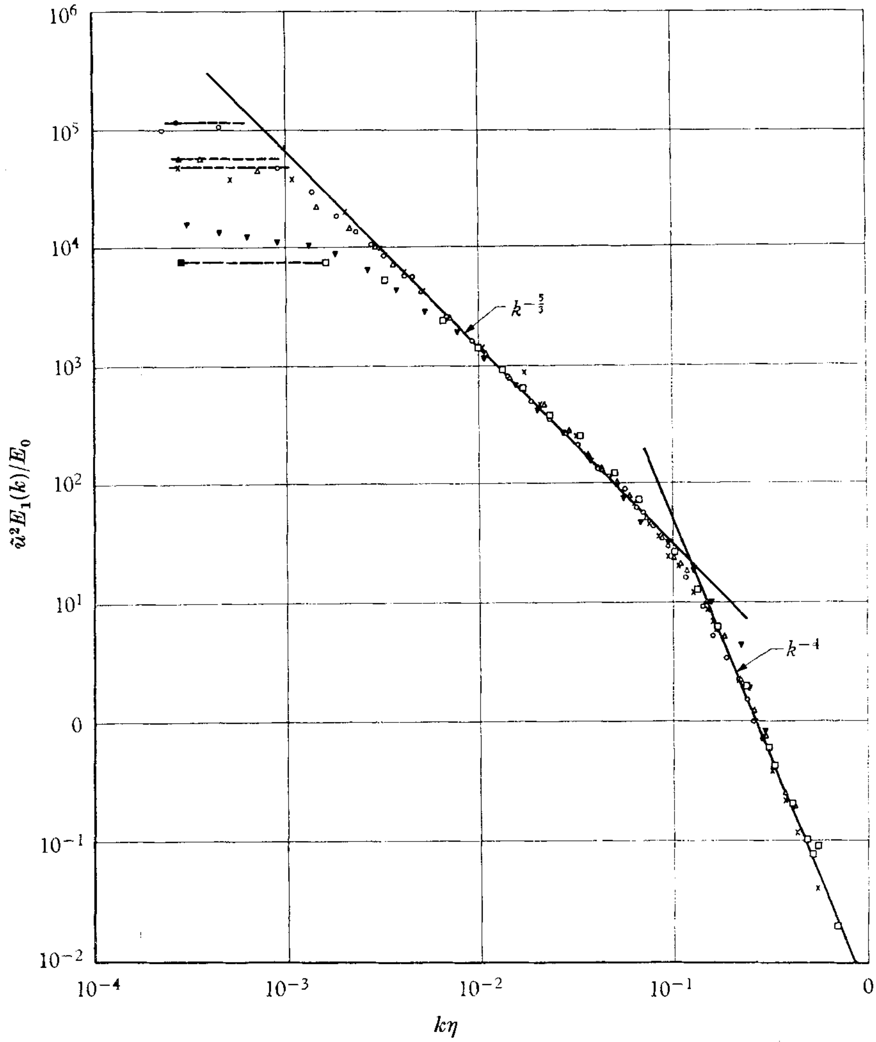

FIGURE 4. The spectra of the stream-wise component of the velocity fluctuation. The solid symbols and dashed line near $k\eta = 0{\cdot}01$ are computed from the realtion $\epsilon = D\tilde{u}^3/L$, with $D = 0{\cdot}4$, and are the estimated $k = 0$ value for the spectra. ○, $Re_L = 1{\cdot}3 \times 10^4$; △, $Re_L = 7{\cdot}5 \times 10^3$; ×, $Re_L = 6{\cdot}5 \times 10^3$; □, $1{\cdot}5 \times 10^3$; ▼, $3{\cdot}2 \times 10^3$ [Laufer 1954 (pipe)].

isotropy; that is, no systematic change of the data with Reynolds number is apparent, and the predictions from E_1 are possible average curves through the E_2 data. For $k\eta < 0{\cdot}03$, however, the E_2 data definitely lie below the isotropic prediction. No extensive interval of constant slope is present in the E_2 data, so that it is impossible to ascribe any particular power law to the data in this region.

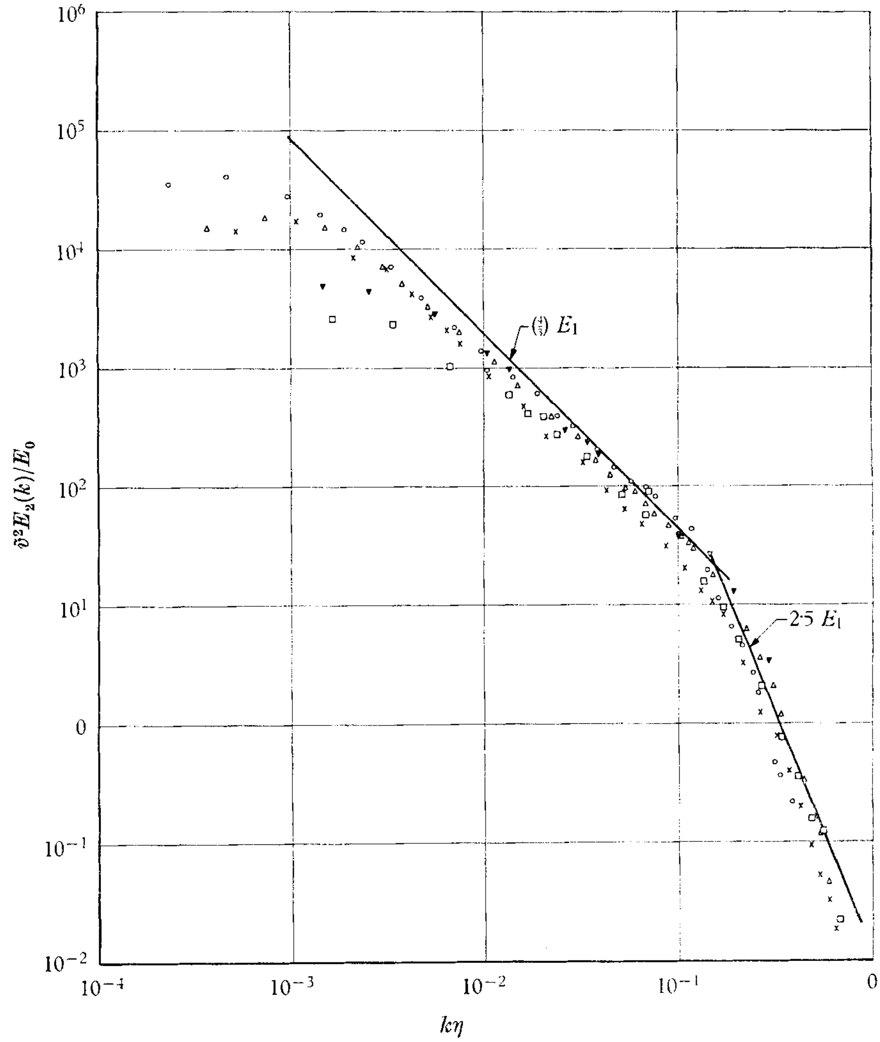

FIGURE 5. The spectra of the cross-stream component of the velocity fluctuation. The two lines, $k^{-\frac{5}{3}}$ and k^{-4}, are related to the lines in figure 4 by the isotropic relationship. Symbols as in figure 4.

7. Conclusions

The data presented here allow conclusions to be drawn on two aspects of grid turbulence: (1) the general features of this turbulence as determined by the large-scale components of the turbulent motion, and (2) the features of the small-scale components of the motion at high Reynolds numbers.

Grid turbulence has been studied extensively at low Reynolds numbers because it is the closest realization of isotropic turbulence. The data described here show that the main features of this turbulence change with Reynolds number only in so far as the flow over the grid does so; i.e. the turbulent energy is proportional to the pressure drop across the grid. The decay data can be fitted with an initial-period decay law ($\tilde{u} \sim 1/x$); $\tilde{u}$ is greater than $\tilde{v}$ for the entire Re_L range; and the spectral shapes at small wave number are independent of Reynolds number. Apparently no new phenomena come into play at large Reynolds numbers, and data taken at much lower Reynolds numbers adequately describe the main features of the flow.

The conclusions that can be drawn from the data obtained to examine Kolmogoroff's theory are not as definite as one would wish. Scales determined from the dissipation rate and the viscosity bring together the large wave-number data for the various Reynolds numbers. The relation between the u' and v' spectra seems to satisfy the condition for isotropy at sufficiently large wave numbers ($k\eta > 0{\cdot}1$). For smaller wave numbers, in the so-called inertial subrange, the relation between the two sets of spectra is not, however, as expected. The u' spectra have the predicted shape, but the v' spectra are not related to the u' spectra through the isotropic relation, and the shape of the v' spectra is not the expected $k^{-\frac{5}{3}}$. The same discrepancy is shown in the data of Laufer (1954) for a pipe flow (included in figure 4) and of Klebanoff (1955) in a boundary layer. Since this discrepancy does not change with Reynolds number, i.e. the region where isotropy prevails does not get larger with increasing Reynolds number, it is unlikely that the discrepancy can be ascribed to excessively small Reynolds numbers. Considering that others (e.g. Gibson 1963; Grant & Moilliet 1962) have obtained isotropy in this region for different kinds of flows at comparable Reynolds numbers, it is more probable that the Kolmogoroff theory concerning the inertial subrange does not apply equally to all flows but depends on the particular mechanism which produced the turbulence. Kolmogoroff himself suggested a modification of the theory that makes the results dependent on the distribution of dissipation in the particular flow. Unfortunately, the above data cannot be used to resolve this question.

The u' spectra obtained here can be used to estimate the minimum Reynolds number, at which an inertial subrange might be expected. If one employs the criterion that the spectral curve should follow along the $-\frac{5}{3}$ slope for at least a factor of two in energy, then a value of $(Re_L)_{\min} = 300$ is obtained.

REFERENCES

Favre, A., Gaviglio, J. & Dumas, R. 1953 *La Rech. Aero.* no. 32.

Gibson, M. M. 1963 *J. Fluid Mech.* **15**, 161.

Grant, H. L. & Moilliet, A. 1962 *J. Fluid Mech.* **13**, 237.

Kistler, A. L. & Vrebalovich, T. 1961 *Bull. Amer. Phys. Soc.* II, **6**, 207.

Klebanoff, P. S. 1955 *NACA Rep.* no. 1247.

Laufer, J. 1954 *NACA Rep.* no. 1174.

Uberoi, M. S. & Kovásznay, L. S. G. 1953 *Quart. J. Appl. Math.* **10**, 375.